Abdominal Imaging

Published online: 24 January 2008

Abdom Imaging (2008) 33:740–743
DOI: 10.1007/s00261-008-9362-1

Struma ovarii: CT findings

Sung Il Jung,[1] Young Jun Kim,[1] Min Woo Lee,[1] Hae Jeong Jeon,[1] Jong-Sun Choi,[2] Min Hoan Moon[3]

[1]Department of Radiology, Konkuk University Hospital, Konkuk University School of Medicine, Seoul, Korea
[2]Department of Pathology, Dongguk University International Hospital, Dongguk University College of Medicine, Goyang, Korea
[3]Department of Radiology, Cheil General Hospital and Women's Healthcare Center, Kwandong University School of Medicine, 1-19 Mookjung-Dong, Jung-Gu, 100-380, Seoul, Korea

Abstract

Background: The purpose of this study was to evaluate computed tomographic findings of struma ovarii.
Methods: Computed tomography (CT) scans of 13 pathologically proven struma ovarii were retrospectively reviewed by two radiologists in consensus. Scans were evaluated for the laterality, size, mass configuration, margins, internal architecture, presence of intracystic high attenuation lesions on precontrast scans, and cyst wall enhancement.
Results: The mean size of the tumors was 11.4 cm (range 4.7–21.0 cm). Mainly cystic (n = 8, 61.5%) or cystic (n = 5, 38.5%) appearance was common to all the tumors. All tumors were unilateral and had smooth margins. The most common internal architecture in the tumors was multicystic architecture (n = 11, 84.6%). Eleven tumors (84.6%) showed a high attenuation lesion in the cyst portion of the mass on precontrast scans and the attenuation ranged from 92.2 to 120.5 Hounsfield units (HU) (mean, 106.8 ± 8.8 HU). The cyst wall showed no (n = 7, 53.8%), moderate (n = 5, 38.5%), or marked (n = 1, 7.7%) enhancement after administration of contrast medium.
Conclusions: On CT scans, struma ovarii appeared most often as a smooth marginated multicystic mass with a high attenuation lesion on precontrast scans and no or moderate cyst wall enhancement.

Key words: Struma ovarii—Neoplasms—Computed tomography—Ovary—Pelvis

Correspondence to: Min Hoan Moon; *email:* moon@radiol.snu.ac.kr

Struma ovarii is an uncommon ovarian tumor composed entirely or predominantly (over 50%) of thyroid tissue with large follicle-containing colloid material [1]. This tumor often accompanies mature cystic teratomas and most cases are benign [2, 3]. However, because these tumors have both solid and cystic components [3–5], it is difficult to differentiate them preoperatively from other ovarian cancers, especially in cases without accompanying mature cystic teratomas.

Computed tomography (CT) is generally accepted as the imaging modality in the evaluation of gynecologic pelvic mass. Some authors have reported radiological findings of struma ovarii; however, most articles have been based on magnetic resonance (MR) imaging and there have been no large-scale studies on the CT findings of struma ovarii [6–11]. The purpose of this study was to characterize the CT appearance of struma ovarii.

Materials and methods

Our study was a retrospective review of all cases of pathologically proven struma ovarii from January 1, 2002 to February 28, 2007.

A total of 27 cases were obtained from a search of the pathology department database in our institution. Histopathologic review of the cases was performed by one of the authors (J.S.C.). Among them, 14 cases were excluded because their CT scans were not available for review; thus, the remaining 13 cases with pre- and post-contrast enhanced CT constituted our study population.

All CT data were obtained using a spiral CT scanner (Hispeed CT/i, General Electric Medical Systems, Milwaukee, WI). Preoperative CT scans were obtained with an average of 6 days before surgery (range, 2–11 days) at a single institution using a single CT scanner. Patients received 130 cc of intravenous contrast material (iopromide, Ultravist 300, Schering, Berlin, Germany) in an

Table 1. Summary of cases

Case No.	Age (Years)	Location	Size (cm)	Mass configuration	Margins	Internal architecture	Intracystic high attenuation lesion (HU)[a]	Cyst wall enhancement
1	41	Left	5.5	Mainly cystic	Smooth	Multicystic	Present (102.4)	Moderate
2	52	Right	10.8	Mainly cystic	Smooth	Multicystic	Present (114.6)	None
3	24	Right	9.5	Mainly cystic	Smooth	Multicystic	Present (110.9)	Moderate
4	50	Right	6.3	Mainly cystic	Smooth	Multicystic	Present (94.4)	Moderate
5	35	Left	4.7	Mainly cystic	Smooth	Multicystic	Present (102.1)	Moderate
6	33	Left	9.4	Mainly cystic	Smooth	Multicystic	Present (120.5)	None
7	27	Right	11.0	Cystic	Smooth	Multicystic	Present (92.2)	None
8	67	Left	8.1	Mainly cystic	Smooth	multicystic	Absent (43.2)	Marked
9	27	Left	21.0	Cystic	Smooth	Unilocular	Absent (29.1)	None
10	51	Left	13.2	Cystic	Smooth	Multicystic	Present (102.8)	None
11	18	Left	20.3	Cystic	Smooth	Multiseptated	Present (108.7)	None
12	24	Right	11.7	Mainly cystic	Smooth	Multicystic	Present (110.6)	Moderate
13	22	Left	16.3	Cystic	Smooth	Multicystic	Present (115.2)	None

[a] We defined an intracystic high attenuation lesion as a lesion in the cystic portion of the mass measuring more than 80 CT HU on precontrast scans. The values in parentheses are the highest values measured in the intracystic high attenuation lesion

antecubital vein via mechanical injector, administered at a rate of 2 cc/sec. Scanning was done before contrast injection and after 130 s of contrast material injection and covered the region from diaphragm to the lower vagina. The scanning parameters included slice thicknesses of 5 mm, reconstruction intervals of 5 mm, and a beam pitch of 1.2.

Computed tomography images were reviewed retrospectively by consensus by two radiologists (S.I.J., M.H.M.) who had 5 and 7 years of experience in gynecologic imaging, respectively. The categories for image analysis were as follows: laterality, size (longest diameter in axial scans), mass configuration (cystic or, mainly cystic with more than two-thirds of the mass), mainly solid with more than two-thirds of the mass or solid), margin (smooth vs. irregular), internal architecture (unilocular, multicystic, multiseptated), presence of an intracystic high attenuation lesion on precontrast scans (we defined an intracystic high attenuation lesion as a lesion in the cystic portion of the mass measuring more than 80 CT Hounsfield units (HU), which was the approximate mean CT value of the normal thyroid [12]), and cyst wall enhancement (moderate or marked). Cyst wall enhancement after administration of contrast medium was assessed relative to enhancement of the normal uterine myometrium; moderate (less than that of myometrium), or marked (greater than that of myometrium).

The CT value differences of the intracystic high attenuation lesion between precontrast and postcontrast scan were compared by use of Wilcoxon's signed rank test. $P < 0.05$ was considered significant.

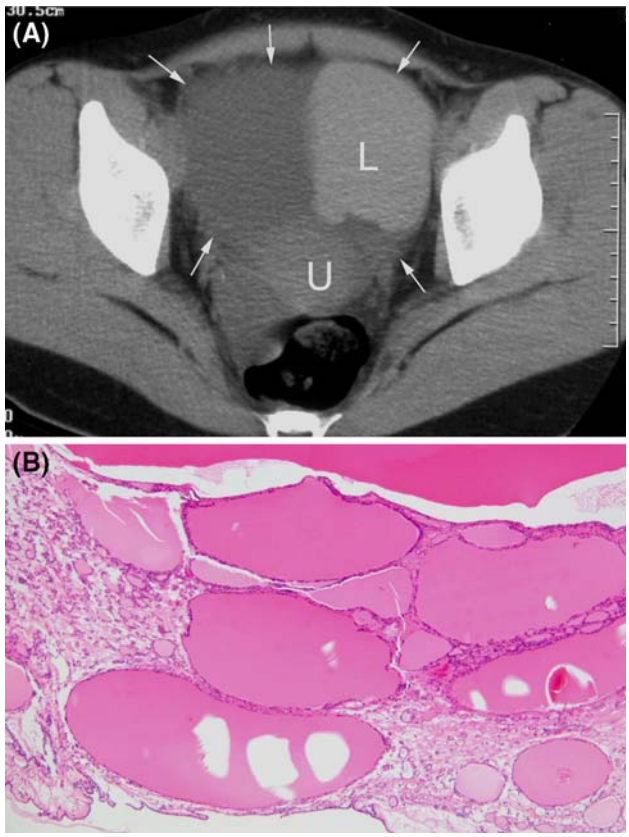

Fig. 1. Struma ovarii in 22-year-old woman. A, Precontrast CT scan shows smooth marginated mass with an internal high attenuation lesion (L) of 115.2 HU in the left ovary (*arrows*). Uterus (*U*). B, Microscopic appearance of a high attenuation lesion in the mass shows multiple thyroid follicles with eosinophilic colloid (original magnification, ×40)

Results

The results are summarized in Table 1. The age of patients ranged from 18 to 67 years (mean 36.2 years). The size of the tumors ranged from 4.7 to 21.0 cm (mean 11.4 cm). Mainly cystic ($n = 8$, 61.5%) or cystic ($n = 5$, 38.5%) appearance was seen in the all tumors; no tumor had a solid appearance (Figs. 1–3). All tumors were unilateral and had smooth margins (Figs. 1–3). The most common internal architecture of the tumors was multicystic architecture ($n = 11$, 84.6%) (Figs. 1–3). Eleven

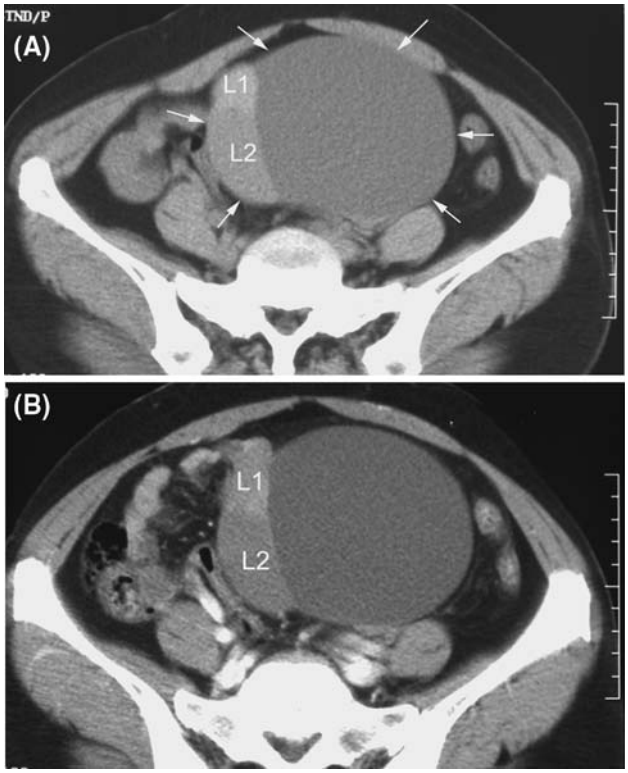

Fig. 2. Struma ovarii in 51-year-old woman. A, Precontrast CT scan shows smooth marginated mass with multiple high attenuation lesions (L1, L2) in the mass (*arrows*), of 106.1 HU and 99.6 HU, respectively. B, Contrast-enhanced CT scan shows no cyst wall enhancement, nor are the lesions significantly enhanced

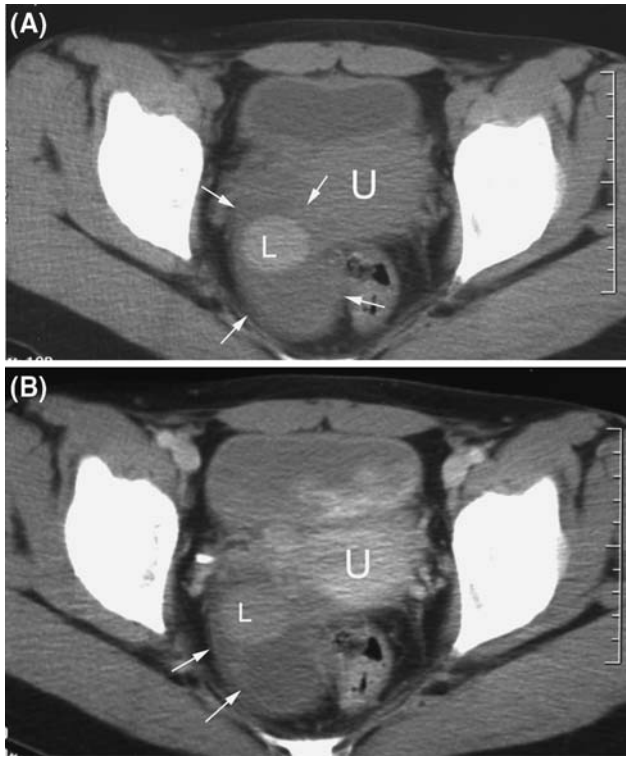

Fig. 3. Struma ovarii in 24-year-old woman. A, Precontrast CT scan shows mainly cystic mass with a central high attenuation lesion (L) of 110.9 HU in the right ovary (*arrows*). Uterus (*U*). B, Contrast-enhanced CT scan shows moderate cyst wall enhancement (*arrows*), but the lesion is not significantly enhanced

tumors (84.6%) showed a high attenuation lesion in the cystic portion of the mass on precontrast CT scans and the attenuation ranged from 92.2 to 120.5 HU (mean, 106.8 ± 8.8 HU) (Figs. 1–3). There was no significant difference for CT value of the lesion between precontrast and postcontrast scan (median, 108.7 vs. 110.2 HU; $P = 0.08$, Wilcoxon's signed rank test).

Cyst wall was moderately ($n = 5$, 38.5%) or markedly ($n = 1$, 7.7%) enhanced after administration of contrast medium (Figs. 3, 4). Seven tumors (53.8%) showed no cyst wall enhancement. Mature cystic teratoma in the contralateral ovary was confirmed in three cases and mucinous cystadenoma in the contralateral ovary was confirmed in one case.

Discussion

Struma ovarii is an uncommon ovarian tumor, constituting only 2.7% of all ovarian teratomas [2]. Although struma ovarii contains thyroid tissue and can be associated with hyperthyroidism, the incidence of hyperthyroidism is only about 5% [13, 14]. Most patients are asymptomatic and are not diagnosed until the development of symptoms of torsion, abdominal distention, or ascites [1, 15]. To our knowledge, it was generally reported that MR findings of the tumor was a multilocular cystic and solid mass with a variable signal intensity within loculi, especially with low signal intensity on T1-weighted images and very low signal intensity on T2-weighted images, or a multicystic mass with a solid component that shows low signal intensity on T1-weighted images and variable signal intensity on T2-weighted images [8, 9, 11]. In those reports, the solid components with low signal intensity on T1- and T2-weighted images corresponded pathologically with gelatinous colloid material.

We found that this tumor was most often a multicystic mass with smooth margins, which coincided well with previous studies [6, 9, 10]. Interestingly, most of our cases showed intracystic high attenuation lesions on precontrast CT images. The lesion was not significantly enhanced on postcontrast CT images and was filled in a loculus or several loculi of the multilocular mass, with no features such as an intracystic protruding nodule or papillary projection. We suggest that the solid component with low signal intensity on T1- and T2-weighted images in previously reported MR imaging might correspond with the high attenuation lesions on precontrast

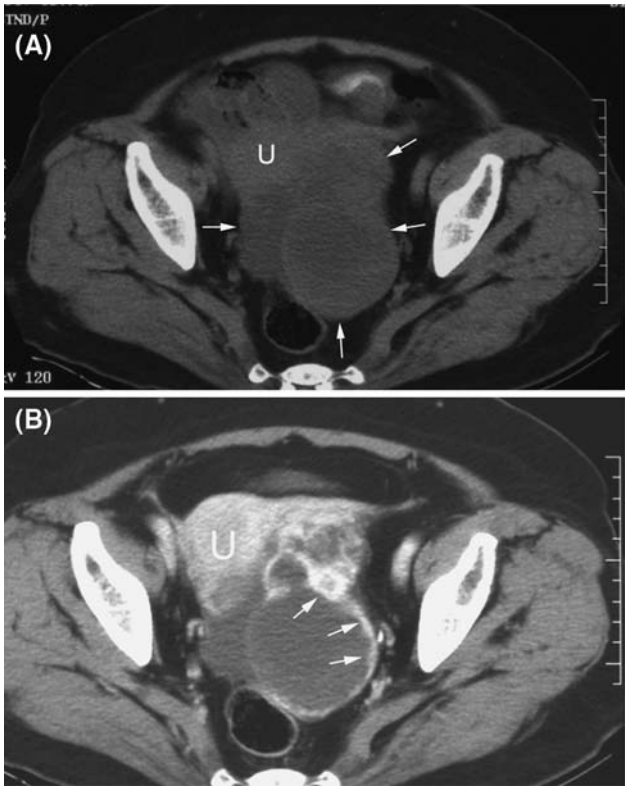

Fig. 4. Struma ovarii in 67-year-old woman. A, Precontrast CT scan shows multicystic mass in the right ovary (*arrows*). Uterus (*U*). B. Contrast-enhanced CT scan shows marked cyst wall enhancement of multicystic mass (*arrows*)

CT scans in our study, which probably consisted of viscid gelatinous colloid material. We suggest that the high HU of colloid material on precontrast CT scans was caused by thyroglobulin and thyroid hormones in the follicle, which have very effective X-ray attenuation [16–18]. However, considering that in two cases there was no high attenuation lesion on the precontrast CT scans, it is likely that the HU of the gelatinous colloid material might be nonspecific and variable depending on the contents of the colloid materials, nevertheless we think that characteristic high attenuation lesion on precontrast CT images can be a differential point from other common epithelial origin tumors as cystadenocarcinoma or cystadenoma, or metastatic tumor. Cyst wall enhancement was absent or moderate in most of our cases. Only in the case with marked cyst wall enhancement was it revealed that the tumor had no tissue other than thyroid, and only severe necrosis on pathological examination.

In conclusion, struma ovarii usually appears as a smooth marginated multicystic mass with a high attenuation lesion on precontrast CT scans and no or moderate cyst wall enhancement.

References

1. Kempers RD, Dockerty MB, Hoffman DL, et al. (1970) Struma ovarii-ascitic, hyperthyroid, and asymptomatic syndromes. Ann Intern Med 72:883–893
2. Outwater EK, Siegelman ES, Hunt JL (2001) Ovarian teratomas: tumor types and imaging characteristics. Radiographics 21:475–490
3. Roth LM, Talerman A (2007) The enigma of struma ovarii. Pathology 39:139–146
4. Roth LM, Talerman A (2006) Recent advances in the pathology and classification of ovarian germ cell tumors. Int J Gynecol Pathol 25:305–320
5. Szyfelbein WM, Young RH, Scully RE (1995) Struma ovarii simulating ovarian tumors of other types. A report of 30 cases. Am J Surg Pathol 19:21–29
6. Dohke M, Watanabe Y, Takahashi A, et al. (1997) Struma ovarii: MR findings. J Comput Assist Tomogr 21:265–267
7. Hahn ST, Park SH, Bahk YW, et al. (1991) Struma ovarii simulating a teratodermoid cyst. Computed tomographic findings in one case. Radiologe 31:89–91
8. Joja I, Asakawa T, Mitsumori A, et al. (1998) Struma ovarii: appearance on MR images. Abdom Imaging 23:652–656
9. Matsuki M, Kaji Y, Matsuo M, et al. (2000) Struma ovarii: MRI findings. Br J Radiol 73:87–90
10. Matsumoto F, Yoshioka H, Hamada T, et al. (1990) Struma ovarii: CT and MR findings. J Comput Assist Tomogr 14:310–312
11. Yamashita Y, Hatanaka Y, Takahashi M, et al. (1997) Struma ovarii: MR appearances. Abdom Imaging 22:100–102
12. Som PM, Curtin HD (2003). Head and neck imaging Philadelphia, PA: Mosby
13. Grandet PJ, Remi MH (2000) Struma ovarii with hyperthyroidism. Clin Nucl Med 25:763–765
14. March DE, Desai AG, Park CH, et al. (1988) Struma ovarii: hyperthyroidism in a postmenopausal woman. J Nucl Med 29:263–265
15. Marcus CC, Marcus SL (1961) Struma ovarii. A report of 7 cases and a review of the subject. Am J Obstet Gynecol 81:752–762
16. Iida Y, Konishi J, Harioka T, et al. (1983) Thyroid CT number and its relationship to iodine concentration. Radiology 147:793–795
17. Imanishi Y, Ehara N, Mori J, et al. (1991) Measurement of thyroid iodine by CT. J Comput Assist Tomogr 15:287–290
18. Imanishi Y, Ehara N, Shinagawa T, et al. (2000) Correlation of CT values, iodine concentration, and histological changes in the thyroid. J Comput Assist Tomogr 24:322–326